Supporting Information for

Interface prompted highly efficient hydrogen evolution of

MoS$_2$/CoS$_2$ heterostructures in wide pH range

Tian Wang,[1] Pu Chang,[2] Zhipeng Sun,[1] Xiaohu Wang,[3] Junguang Tao[2,] and Lixiu Guan[1,*]*

[1]School of Science, Hebei University of Technology, Tianjin 300401, China

[2]School of Materials Science and Engineering, Hebei University of Technology, Tianjin 300132, China

[3]Ulanqab Key Laboratory of graphite (graphene) new materials, Rising Graphite Applied Technology Research Institute, Ulanqab, Inner Mongolia, 013650, China

Material Synthesis:

Synthesis of MoS$_2$/CoS$_2$ heterostructure on carbon cloth (CC): CC was immersed in acetone, ethanol and deionized (DI) water for ultrasonically cleaning of 30 min in each step. At first, 0.55 g Co(NO$_3$)$_2$·6H$_2$O and 1.30 g 2-methylimidazole (C$_4$H$_6$N$_2$) were uniformly dissolved in 40 mL water, respectively. Subsequently, a piece of treated CC (2×3 cm^2) was immersed in a mixed purple solution consisting of the above two solutions at room temperature for 5 h. The purple CC at the end of the reaction was repeatedly rinsed with ethanol and dried overnight to obtain cobalt-based metal-organic framework on CC (Co-MOF/CC).

Secondly, the prepared Co-MOF/CC was immersed into a 50 mL (ethanol: DI water = 3:2) solution containing 0.91 g sodium molybdate (Na$_2$MoO$_4$) and etched at 100 °C for 3 h. After etching, the samples were washed by ethanol and dried overnight to obtain CoMoO$_4$/CC.

At last, the MoS$_2$/CoS$_2$ heterostructure was prepared by simple one-

step calcination at 400 °C for 5 h under Ar atmosphere, where 1 g thiourea powder and $CoMoO_4$/CC precursors were placed in the upstream and downstream of the tube furnace, respectively. The mass loading of MoS_2/CoS_2 on CC was calculated to be ~2.05 mg cm^{-2}.

Synthesis of CoS$_2$ on CC: The conditions remained the same except for the replacement of 0.91 g sodium molybdate with 0.69 g of $Co(NO_3)_2 \cdot 6H_2O$ in the preparation of $CoMoO_4$ step. The mass loading of CoS_2 on CC was calculated to be ~1.97 mg cm^{-2}.

Synthesis of MoS$_2$ on CC: The MoS_2 was prepared on CC using a simple hydrothermal method. A piece of treated CC (2×3 cm^2) substrate was immersed in 40 mL aqueous solution composed of 0.25 g Na_2MoO_4 and 0.5 g TAA. Subsequently, the solution was transferred into a 50 mL Teflon-lined stainless autoclave and heated to 200 °C for 20 h. The prepared sample was washed with ethanol and dried at 60 °C to obtain the MoS_2 on CC. The mass loading of MoS_2 on CC was calculated to be ~2.08 mg cm^{-2}.

Preparation of Pt/C on CC: The commercial Pt/C (20 wt %, Aladdin) and IrO_2 (99%, Aladdin) was drop-casted on CC using catalyst ink. The catalyst ink was obtained by dispersing Pt/C uniformly in a solution containing 0.5 mL ethanol and 50 μL Nafion. The mass loading of Pt/C was calculated to be ~2.0 mg cm^{-2}.

Electrochemical measurements: The electrochemical performance was tested with a three-electrode configuration using LK2010A

electrochemical workstation (Tianjin, China). Nitrogen saturated solutions of 0.5 M H_2SO_4 and 1.0 M KOH were used as acidic and alkaline electrolytes, respectively. The saturated calomel electrode (SCE) and Ag/AgCl were used as the reference electrode in 1 M KOH and 0.5 M H_2SO_4, respectively. The obtained catalysts on carbon cloth (CC) and a graphite rod were directly used as the working electrode and the counter electrode, respectively. The linear sweep voltammetry (LSV) curves were performed at a scan rate of 5 mV s^{-1} with *iR* compensation. The electrochemical impedance spectroscopy (EIS) measurements were carried out to obtain the R_{ct} in the frequency range of 100 kHz ~ 0.01 Hz with AC amplitude of 5 mV at the overpotential of 100 mV.

Electrochemical active surface area (ECSA) calculation: The double layer capacitance (C_{dl}) was evaluated according to the following equation: $C_{dl} = \Delta j/2v$, where Δj is the current density difference between anode and cathode at the potential corresponding to 0.520 V and v is the scan rate (Fig. S8). Subsequently, the ECSA was estimated from the C_{dl} according to ECSA = C_{dl}/C_s, which C_s is the specific capacitance.

Table S1. ΔG_{H^*} values for various site on 2H-MoS$_2$, CoS$_2$ and 2H-MoS$_2$/CoS$_2$.

Site	Gibbs free energy ΔG_{H^*} (eV)	
	Acidic	Alkaline
2H-MoS$_2$-Mo	2.38	3.97
2H-MoS$_2$-S	2.01	4.43
CoS$_2$-S	-4.10	-6.64
CoS$_2$-Co	0.36	0.61
HS-Co	-0.08	-0.25
HS-Mo	0.39	0.48
HS-S(MoS$_2$)	0.71	1.67
HS-S(CoS$_2$)	0.30	0.52

Table S2. ΔG_{H^*} values for various site on 2H-MoS$_2$, CoS$_2$ and 1T-MoS$_2$/CoS$_2$.

Site	Gibbs free energy ΔG_{H^*} (eV)	
	Acidic	Alkaline
1T-MoS$_2$-Mo	-1.01	2.33
1T-MoS$_2$-S	-0.86	0.31
CoS$_2$-S	-4.10	-6.64
CoS$_2$-Co	0.36	0.61
HS-Co	-0.20	0.01
HS-Mo	-0.85	-1.42
HS-S(MoS$_2$)	-0.80	-1.50
HS-S(CoS$_2$)	-0.07	-0.39
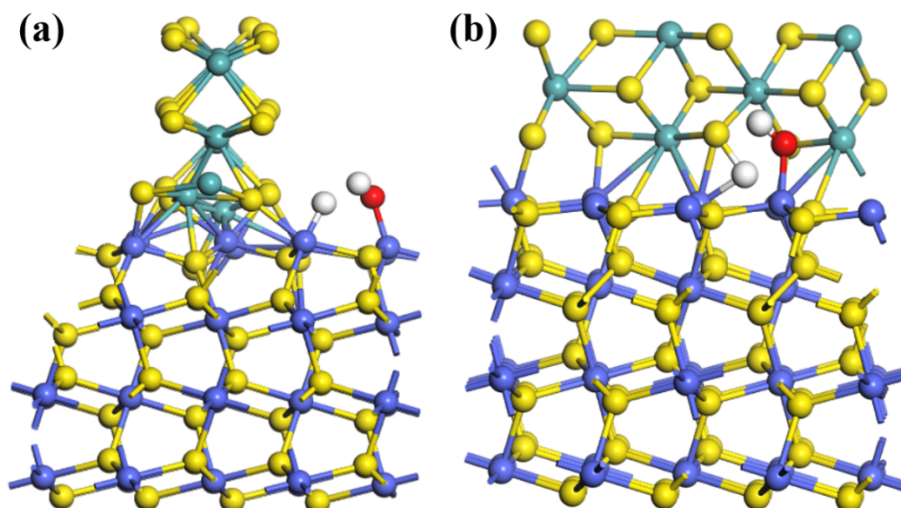
Fig. S1. The OH^- adsorption configurations on Co sites of 2H-MoS$_2$/CoS$_2$ (a) and 1T-MoS$_2$/CoS$_2$ (b). The cyan, yellow blue white and red balls represent Mo, S, Co H and O atoms, respectively.
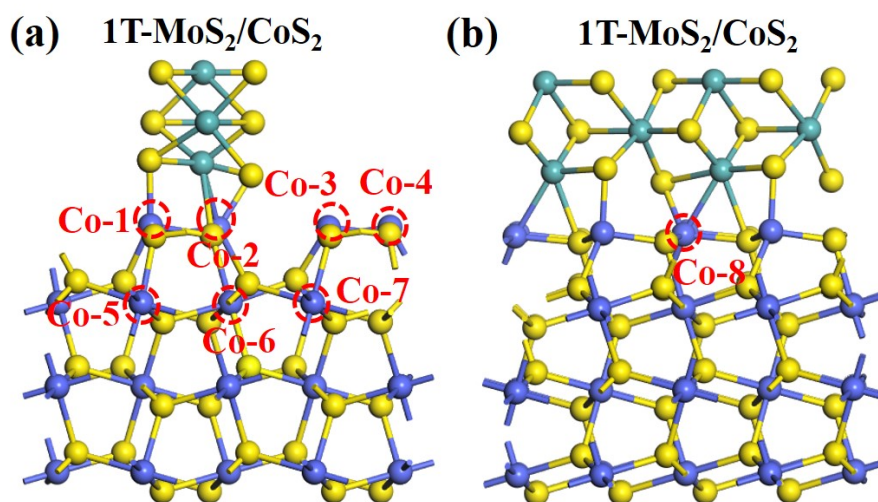

Fig. S2. The H adsorption configurations on different Co sites of 1T-MoS$_2$/CoS$_2$ from different view angles (a) and (b). The cyan, yellow and blue balls represent Mo, S and Co atoms, respectively.
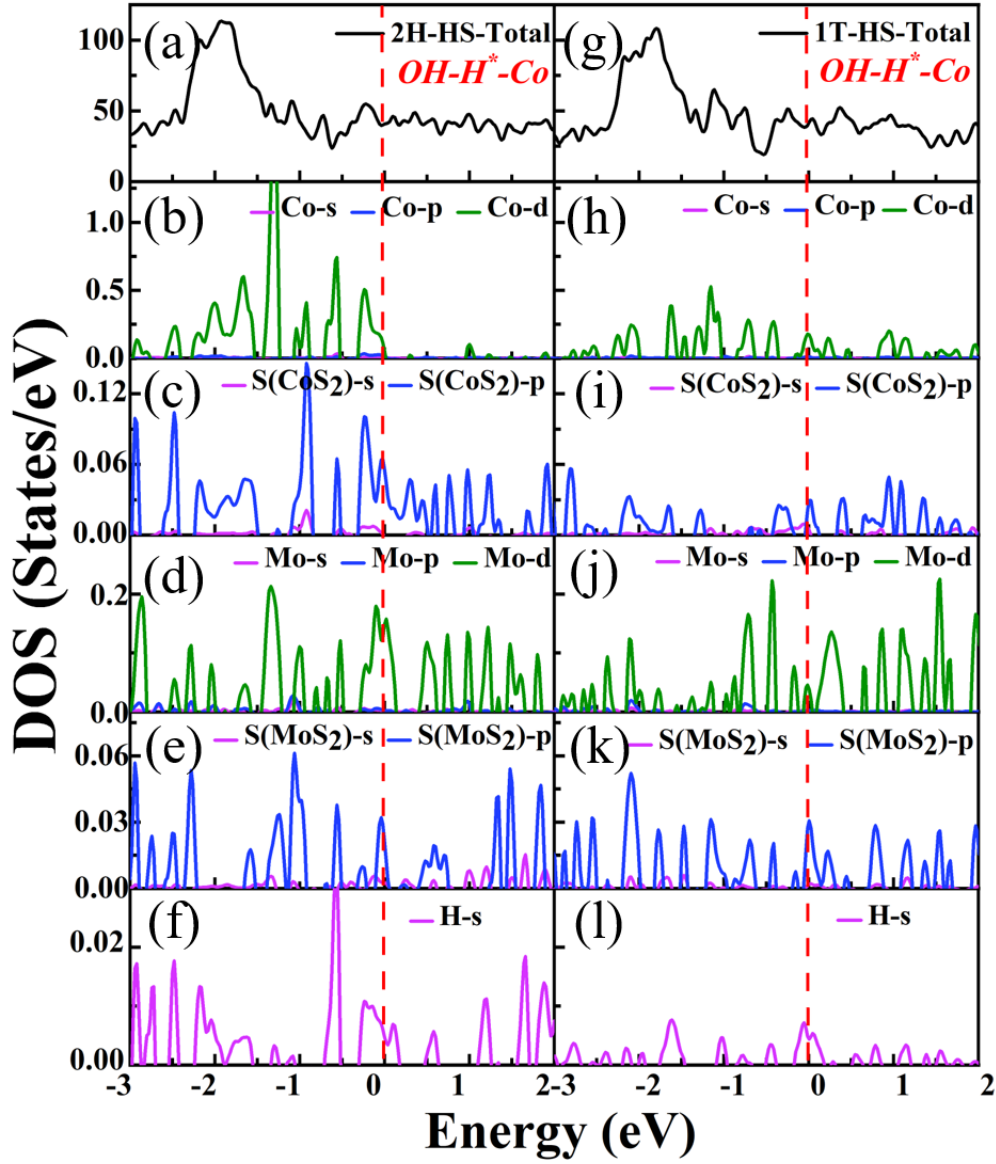
Fig. S3. DOS spectra of OH adsorption on Co sites for 2H-MoS$_2$/CoS$_2$ (a-f) and 1T-MoS$_2$/CoS$_2$ (g-l). (b-f) and (h-l) are the corresponding DOS spectra for Co, S(COS$_2$), Mo, S(MoS$_2$) and H atoms, respectively. The purple, blue and green curves are *s*, *p* and *d* orbitals of the corresponding atoms. The E$_F$ is indicated by a red dashed line.
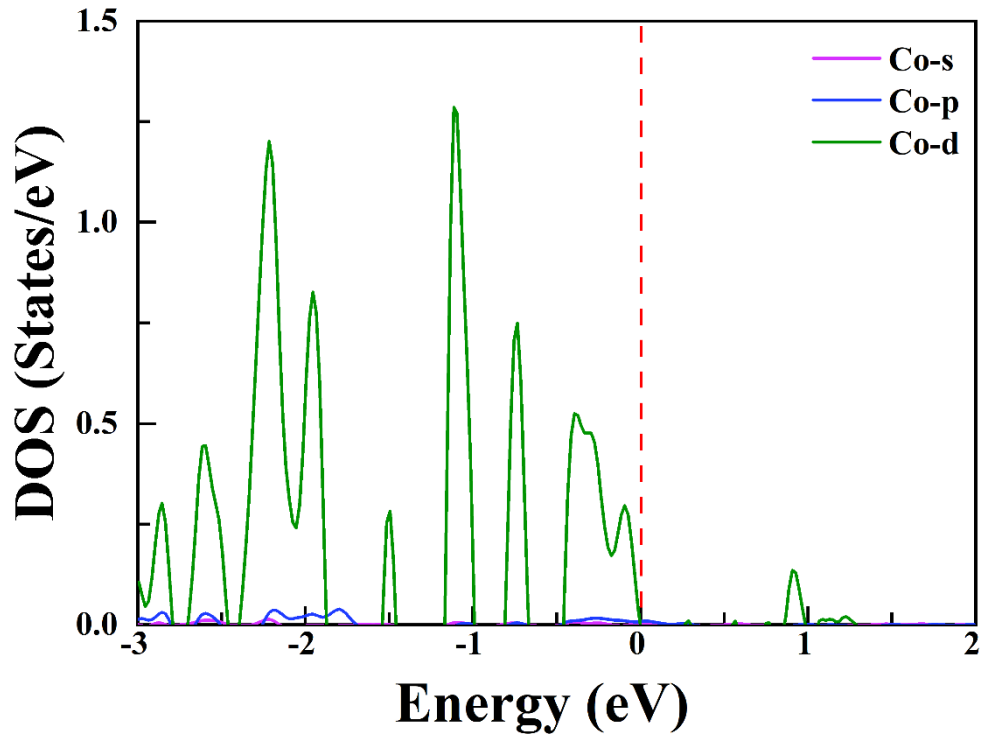
Fig. S4. DOS spectra of internal Co atom. The purple, blue and green curves are *s*, *p* and *d* orbitals of the Co atom. The E_F is indicated by the red dashed line.
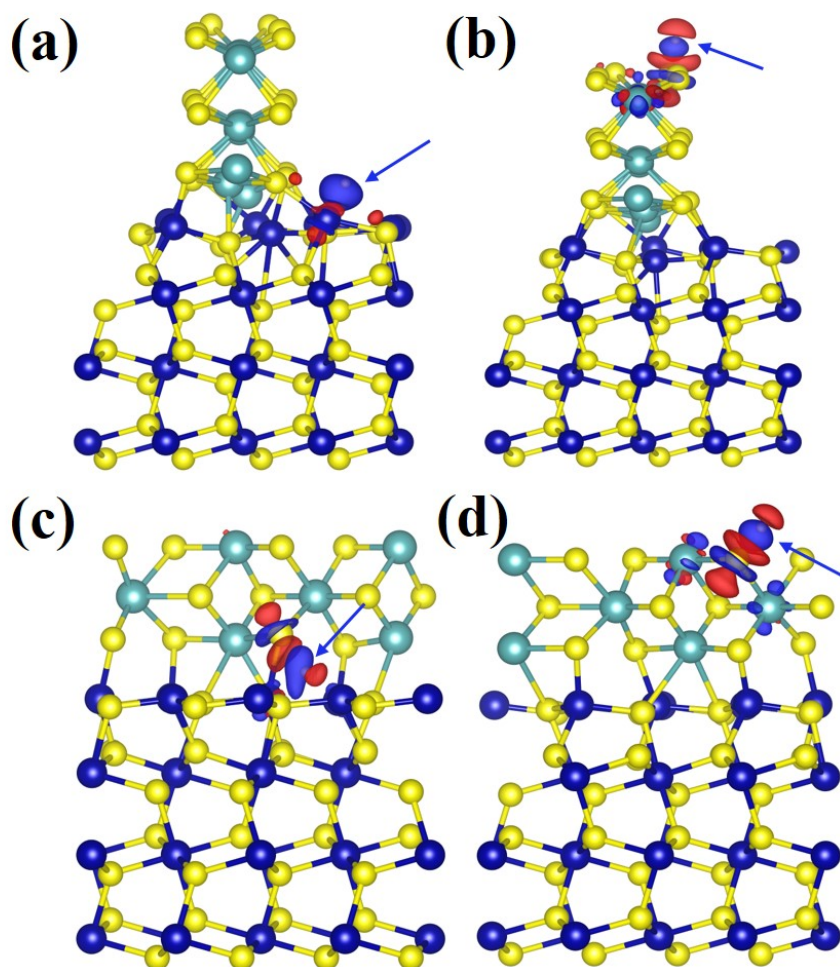
Fig. S5. Differential charge density plots. (a)-(b) are for Co and S(MoS$_2$) site adsorption on 2H-HS. (c)-(d) are the Co and S(MoS$_2$) adsorption configurations on 1T-HS. The blue and red region denote the electron accumulation and depletion, respectively. The isosurface value is 0.005 e Å^{-3}. The blue arrows highlight the electron aggregation phenomenon in the corresponding configurations.
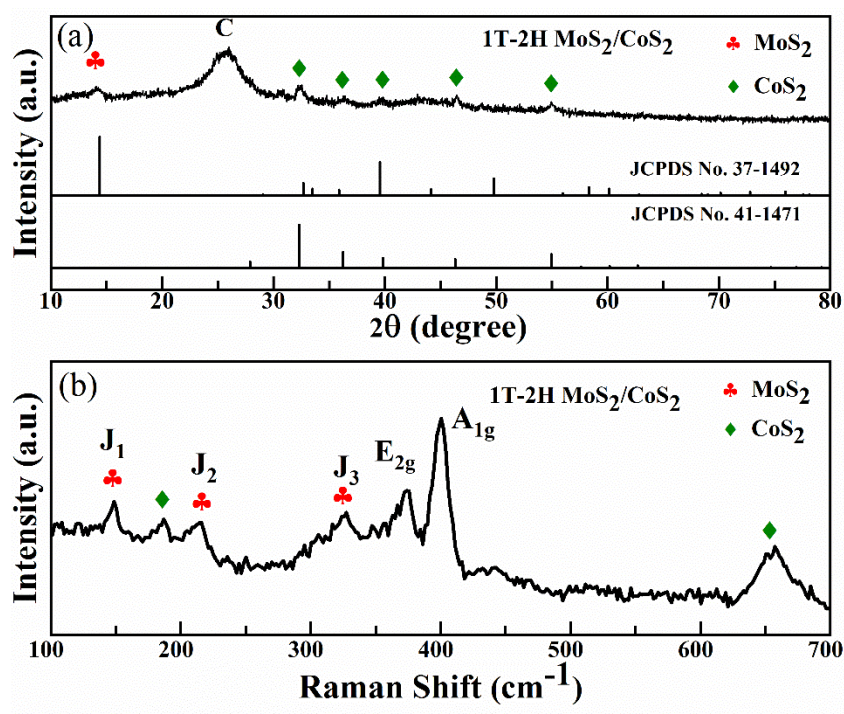
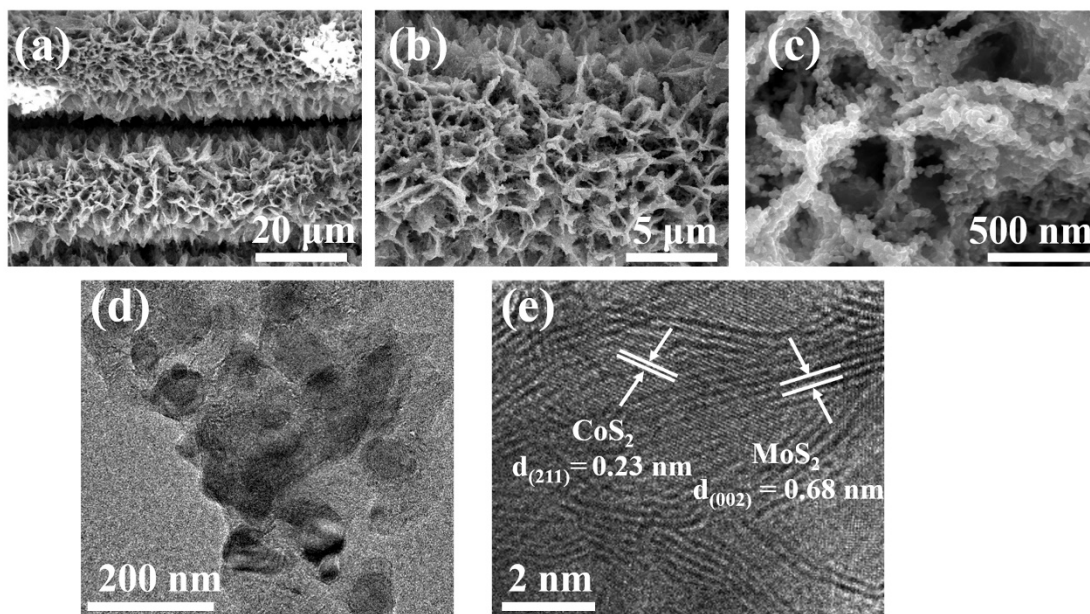Fig. S6. (a) XRD pattern and Raman spectra (b) of 1T-2H MoS_2/CoS_2.

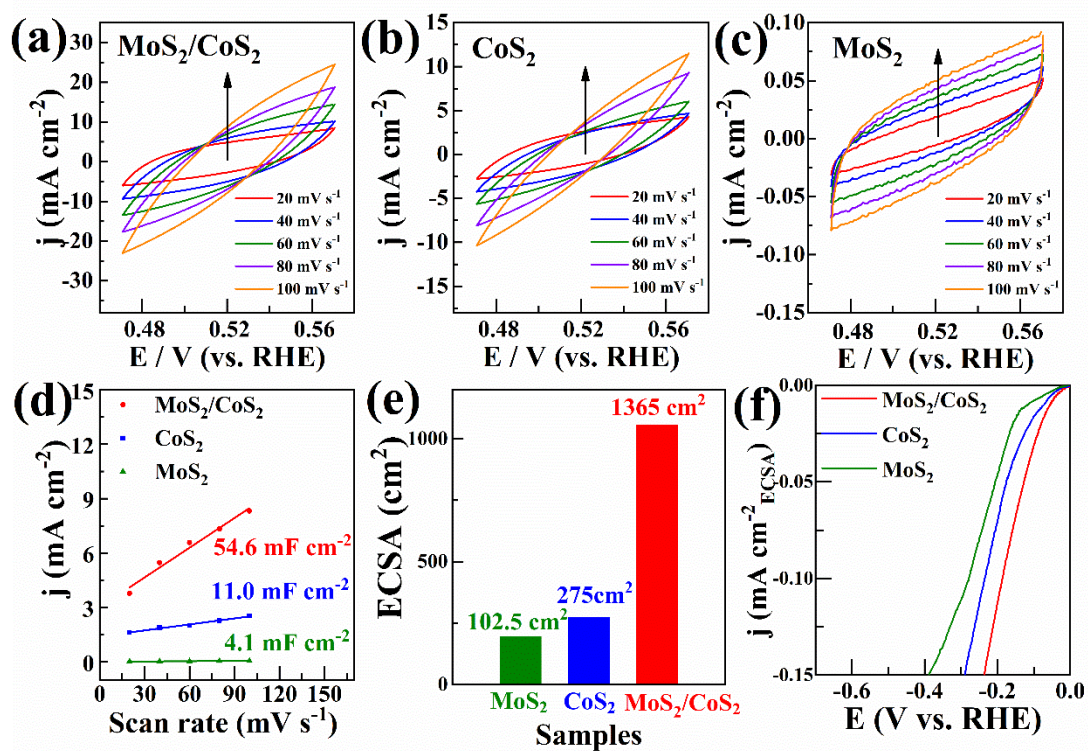Fig. S7. SEM (a-c), TEM (d) and HRTEM (e) images of MoS_2/CoS_2.

Fig. S8. (a-c) CV curves in double layer region (0.47-0.57 V *vs*. RHE), (d) electrochemical double-layer capacitances, (e) electrochemical active surface area and (f) specific activities normalized by ECSA for MoS_2/CoS_2, CoS_2 and MoS_2 at different scan rates (20~100 mV S^{-1}), respectively.
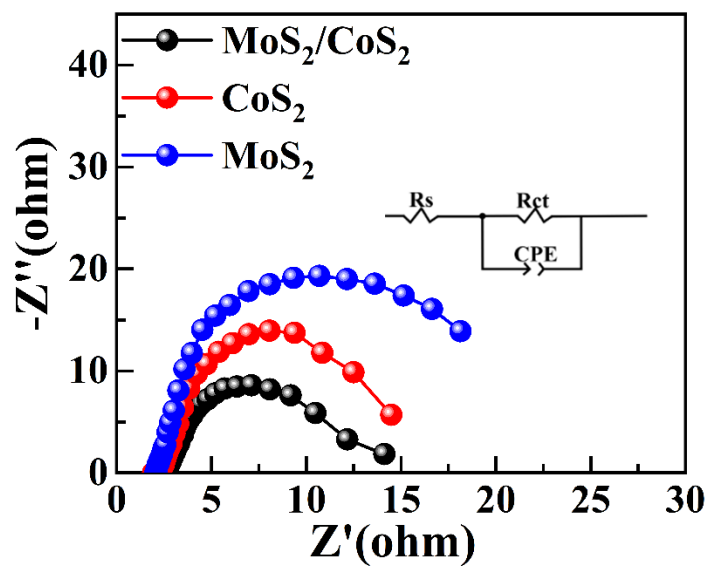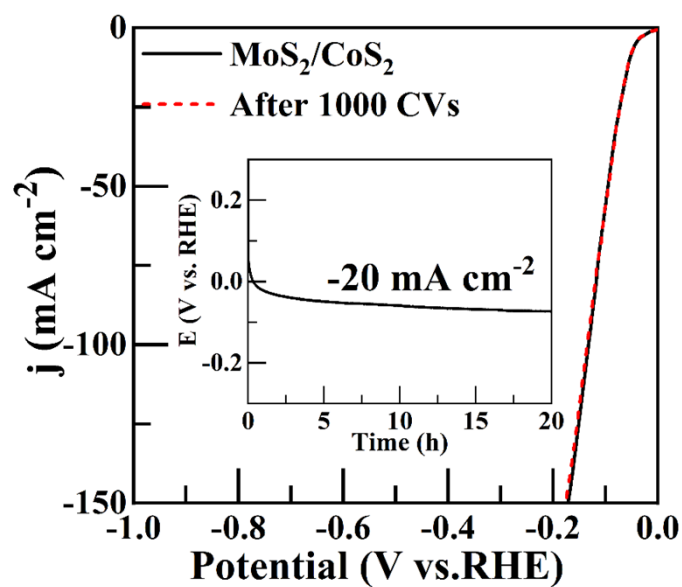
Fig. S9. Nyquist plots of MoS2/CoS2, CoS2, and MoS2.

Fig. S10. Polarization curves of MoS_2/CoS_2 before and after 1000 CV cycles. Inset shows the chronoamperometry tests of MoS_2/CoS_2 at 20 mA cm^{-2} for 20 h.